小山工業高等専門学校研究紀要
第 42 号 (2010) 59－ 64

Dynamic Response of a Nonlinear Vehicle Model

Qin Zhu
Dept. of Mechanical Engineering
Oyama National College of Technology
zhu@oyama-ct.ac.jp

Shan Liang
Automation Academy
Chongqin University
lightsun@cqu.edu.cn

Abstract

In this research, the dynamic responses of a seven-degree-of-freedom ground vehicle model are investigated. It is assumed that the vehicle is subjected to sinusoid disturbance of the road and the nonlinearity is introduced by the suspensions and tires. The numerical results show that the chaotic vibration can be induced by the disturbance and it is found that the chaos is not sensitive to the variation of damping coefficients of the system.

I. INTRODUCTION

Since the disturbance from road may induce uncomfortable shake and noise in the ground vehicle, it is very important to study the dynamic behavior of the automobile. The vibration of the quarter-car model or half-car model has received much attention [1]-[3]. In recent years, the full nonlinear ground vehicle model with seven-degree-of-freedom becomes the research object for dynamic response because the heave, pitch and roll motions of the sprung mass can be investigated with this model. Zhu and Ishitobi have studied the chaotic motion of a full nonlinear ground vehicle model [4]. The periodic response, chaotic response were reported. However, the dynamic response of the model under excitation of the relatively large amplitude was not discussed.

In the present investigation, the frequency response to excitation with large amplitude is studied and the effects of damping coefficients on the chaotic responses of the considered system are investigated. The numerical results show that the chaos of the system is not sensitive to the variation of damping coefficients.

II. MATHEMATICAL MODEL

The nonlinear seven-degree-of-freedom ground vehicle model is shown in Fig. 1 [4]. It is assumed that the sprung mass can have the heave, pitch and roll motions while every unsprung masse can only move up and down.

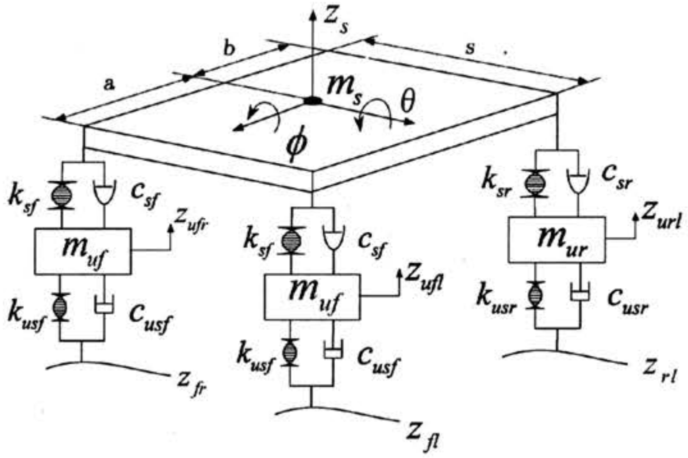

Fig. 1. Nonlinear vehicle model with 7-DOF

Nomenclature

m_s	Sprung mass	$c_{cuf\ell}$, c_{cufr}	Damping coefficient of front suspension
I_ϕ	Roll axis moment of inertia	$c_{cdf\ell}$, c_{cdfr}	Damping coefficient of front suspension
I_θ	Pitch axis moment of inertia	$c_{cur\ell}$, c_{curr}	Damping coefficient of rear suspension
m_{uf}	Front unsprung mass	$c_{cdr\ell}$, c_{cdrr}	Damping coefficient of rear suspension
m_{ur}	Rear unsprung mass	k_{usf}, k_{usr}	Tire spring stiffness
k_{sf}	Front suspension spring stiffness	c_{usf}, c_{usr}	Damping coefficient of tire
k_{sr}	Rear suspension spring stiffness	n_{usf}, n_{usr}	Nonlinear coefficient of tire spring
n_{sf}, n_{sr}	Nonlinear coefficient of suspension spring	Z_{fl}, Z_{fr}, Z_{rl}, Z_{rr}	Forcing function

The suspensions between the sprung mass and unsprung masses are modeled as nonlinear spring and nonlinear damper elements. The dynamic forces of the nonlinear spring are assumed as

$$F_{sij} = k_{sij}\,\mathrm{sgn}(\Delta_{sij})\,|\Delta_{sij}|^{n_{sij}} \qquad (i = f, r, \quad j = \ell, r). \tag{1}$$

where the subscript $i = f, r$ indicates front and rear while the subscript $j = \ell, r$ indicates left and right. The Δ_{sij} is the deformation of the spring and sgn($\cdot$) is the signum function.

The nonlinear damping forces of front and rear suspensions are described by

$$F_{cij} = c_{si}\,\dot{\Delta}_{uij} \qquad (i = f, r, \quad j = \ell, r), \tag{2}$$

where $\dot{\Delta}_{uij}$ is the relative velocity between the extremes of the damper. The damping coefficient c_{si} is expressed by

$$c_{si} = \begin{cases} c_{sui} & \dot{\Delta}_{uij} \geq 0 \\ c_{sdi} & \dot{\Delta}_{uij} < 0 \end{cases} \qquad (i = f, r, \quad j = \ell, r), \tag{3}$$

where c_{sui} and and c_{sdi} are damping coefficients for tension and compression, respectively.

The nonlinear spring force of tire is also simplified as

$$F_{usij} = k_{usi}\,\mathrm{sgn}(\Delta_{usij})\,|\Delta_{usij}|^{n_{usi}} \qquad (i = f, r, \quad j = \ell, r). \tag{4}$$

where Δ_{usij} is the deformation and n_{usi} is the nonlinear coefficient of the tire spring.

The damping of the tires is assumed to be viscous

$$F_{ucij} = c_{usi}\,\dot{\Delta}_{usij}. \tag{5}$$

where $\dot{\Delta}_{usij}$ is the relative velocity of extremes of the model of tires.

The the road disturbance are expressed as

$$\begin{aligned} z_{fr} &= A\sin(2\pi f t), & (6)\\ z_{fl} &= A\sin(2\pi f t + \beta), & (7)\\ z_{rr} &= A\sin(2\pi f t + \alpha), & (8)\\ z_{rl} &= A\sin(2\pi f t + \alpha + \beta). & (9) \end{aligned}$$

where α and β indicate the time delay of the forcing functions. Thus, the equations of motion can be formulated.

Sprung mass:

$$\begin{aligned} m_s\ddot{z}_s &= -F_{sf\ell} - F_{cf\ell} - F_{sfr} - F_{cfr} - F_{sr\ell} - F_{cr\ell} - F_{srr} - F_{crr} - m_s g, & (10)\\ I_\phi\ddot{\phi} &= \Big(-F_{sf\ell} - F_{cf\ell} + F_{sfr} + F_{cfr} - F_{sr\ell} - F_{cr\ell} + F_{srr} + F_{crr}\Big)\frac{s}{2}\cos\phi, & (11)\\ I_\theta\ddot{\theta} &= \Big(F_{sf\ell} + F_{cf\ell} + F_{sfr} + F_{cfr}\Big)a\cos\theta - \Big(F_{sr\ell} + F_{cr\ell} + F_{srr} + F_{crr}\Big)b\cos\theta, & (12) \end{aligned}$$

Unsprung masses:

$$\begin{aligned} m_{uf}\ddot{z}_{uf\ell} &= F_{sf\ell} + F_{cf\ell} - F_{usf\ell} - F_{ucf\ell} - m_{uf}g, & (13)\\ m_{uf}\ddot{z}_{ufr} &= F_{sfr} + F_{cfr} - F_{usfr} - F_{ucfr} - m_{uf}g, & (14) \end{aligned}$$

$$\begin{aligned} m_{ur}\ddot{z}_{ur\ell} &= F_{sr\ell} + F_{cr\ell} - F_{usr\ell} - F_{ucr\ell} - m_{ur}g, & (15)\\ m_{ur}\ddot{z}_{urr} &= F_{srr} + F_{crr} - F_{usrr} - F_{ucrr} - m_{ur}g. & (16) \end{aligned}$$

The forces to the sprung mass in Eqs. (10)-(12) can be calculated as

$$\begin{aligned} F_{sf\ell} &= 100^{(n_{sf}-1)}k_{sf}\,\mathrm{sgn}\,(\Delta_{uf\ell} - \Delta_{sf})\,|\Delta_{uf\ell} - \Delta_{sf}|^{n_{sf}}, & (17)\\ F_{sfr} &= 100^{(n_{sf}-1)}k_{sf}\,\mathrm{sgn}\,(\Delta_{ufr} - \Delta_{sf})\,|\Delta_{ufr} - \Delta_{sf}|^{n_{sf}}, & (18)\\ F_{cf\ell} &= c_{sf}\dot{\Delta}_{uf\ell}, & (19)\\ F_{cfr} &= c_{sf}\dot{\Delta}_{ufr}, & (20)\\ F_{sr\ell} &= 100^{(n_{sr}-1)}k_{sr}\,\mathrm{sgn}\,(\Delta_{ur\ell} - \Delta_{sr})\,|\Delta_{ur\ell} - \Delta_{sr}|^{n_{sr}}, & (21)\\ F_{srr} &= 100^{(n_{sr}-1)}k_{sr}\,\mathrm{sgn}\,(\Delta_{urr} - \Delta_{sr})\,|\Delta_{urr} - \Delta_{sr}|^{n_{sr}}, & (22)\\ F_{cr\ell} &= c_{sr}\dot{\Delta}_{ur\ell}, & (23)\\ F_{crr} &= c_{sr}\dot{\Delta}_{urr}, & (24) \end{aligned}$$

where

$$\begin{aligned} \Delta_{uf\ell} &= \frac{s}{2}\sin\phi - a\sin\theta + z_s - z_{uf\ell}, & (25)\\ \Delta_{ufr} &= -\frac{s}{2}\sin\phi - a\sin\theta + z_s - z_{ufr}, & (26) \end{aligned}$$

$$\Delta_{ur\ell} = \frac{s}{2}\sin\phi + b\sin\theta + z_s - z_{ur\ell}, \tag{27}$$

$$\Delta_{urr} = -\frac{s}{2}\sin\phi + b\sin\theta + z_s - z_{urr}, \tag{28}$$

$$\Delta_{sr} = \left[\frac{a}{100^{(n_{sr}-1)}k_{sr}}\left(\frac{m_s g}{2(a+b)}\right)\right]^{\frac{1}{n_{sr}}}, \tag{29}$$

$$\Delta_{sf} = \left[\frac{b}{100^{(n_{sf}-1)}k_{sf}}\left(\frac{m_s g}{2(a+b)}\right)\right]^{\frac{1}{n_{sf}}}. \tag{30}$$

The forces related to the unsprung mass in Eqs. (13)-(16) are expressed as

$$F_{usf\ell} = 100^{(n_f-1)}k_{usf}\,\mathrm{sgn}\,(\Delta_{usf\ell} - \Delta_{suf})\,|\Delta_{usf\ell} - \Delta_{suf}|^{n_{usf}}, \tag{31}$$

$$F_{usfr} = 100^{(n_f-1)}k_{usf}\,\mathrm{sgn}\,(\Delta_{usfr} - \Delta_{suf})\,|\Delta_{usfr} - \Delta_{suf}|^{n_{usf}}, \tag{32}$$

$$F_{ucf\ell} = c_{usf}\dot{\Delta}_{usf\ell}, \tag{33}$$

$$F_{ucfr} = c_{usf}\dot{\Delta}_{usfr}, \tag{34}$$

$$F_{usr\ell} = 100^{(n_r-1)}k_{usr}\,\mathrm{sgn}\,(\Delta_{usr\ell} - \Delta_{sur})\,|\Delta_{usr\ell} - \Delta_{sur}|^{n_{usr}}, \tag{35}$$

$$F_{usrr} = 100^{(n_r-1)}k_{usr}\,\mathrm{sgn}\,(\Delta_{usrr} - \Delta_{sur})\,|\Delta_{usrr} - \Delta_{sur}|^{n_{usr}}, \tag{36}$$

$$F_{ucr\ell} = c_{usr}\dot{\Delta}_{usr\ell}, \tag{37}$$

$$F_{ucrr} = c_{usr}\dot{\Delta}_{usrr}. \tag{38}$$

where

$$\Delta_{usf\ell} = z_{uf\ell} - A\sin(\omega t + \beta), \tag{39}$$

$$\Delta_{usfr} = z_{ufr} - A\sin(\omega t), \tag{40}$$

$$\Delta_{usr\ell} = z_{ur\ell} - A\sin(\omega t + \alpha + \beta), \tag{41}$$

$$\Delta_{usrr} = z_{urr} - A\sin(\omega t + \alpha), \tag{42}$$

$$\Delta_{sur} = \left[\frac{g}{100^{(n_r-1)}k_{sur}}\left(\frac{m_s a}{2(a+b)} + m_{ur}\right)\right]^{\frac{1}{n_{usr}}}, \tag{43}$$

$$\Delta_{suf} = \left[\frac{g}{100^{(n_f-1)}k_{suf}}\left(\frac{m_s b}{2(a+b)} + m_{uf}\right)\right]^{\frac{1}{n_{usf}}}. \tag{44}$$

III. Numerical results

Because of strong non-linearity in the differential equations (10)-(16), the dynamic responses of the system is studied numerically. The frequency-response diagram and Poincaré map were used to trace the chaos [5]. The parameters of the physic structure of the system is listed in Table I [4] and were used in the numerical study .

The frequency response diagram is often used to predict the forcing frequency which is possible related to chaotic response. By observing an unstable region in the frequency response diagram and finding the corresponding frequencies, the ones which are possibly leading to chaotic response can be obtained. Because the dynamic response of the mathematic model under relatively large forcing amplitude is to be investigated in this research, the amplitude of the forcing function is chosen as $A = 0.08$ m which is greater than one used in reference [4].

Fig. 2 represents the frequency response diagrams of the heave, roll and pitch motion of sprung mass and heave motion of unsprung mass in front-left corner as the forcing frequency of the sinusoid road disturbance is slowly increased and then slowly decreased. The diagrams were obtained by calculating the responses of the system in the range of $0.01 \le f \le 15$ Hz with an increment of the frequency $\Delta f = 0.001$ Hz. In Fig. 2(a)~Fig. 2(h), the vertical axis is defined as the maximum absolute value of the amplitude of the displacement, and the horizontal axis is defined as the frequency of the sinusoid road disturbance.

The frequency response diagram of the heave motion for the sprung mass is shown in Figs. 2(a) and (b). As the forcing

TABLE I

PARAMETERS OF THE SYSTEM

m_s	1500 kg	I_ϕ	460 kg-m	I_θ	2160 kg-m	m_{uf}	59 kg
m_{ur}	59 kg	k_{sf}	35000 N/m	k_{sr}	38000 N/m	n_{sf}, n_{sr}	1.5
$c_{cuf\ell}$, c_{cufr}	1000 N/m/s	$c_{cdf\ell}$, c_{cdfr}	720 N/m/s	$c_{cur\ell}$, c_{curr}	1000 N/m/s	$c_{cdr\ell}$, c_{cdrr}	720 N/m/s
k_{usf}, k_{usr}	190000 N/m	c_{usf}, c_{usr}	10 N/m/s	n_f, n_r	1.25	a	1.4 m
b	1.7 m	s	3 m				

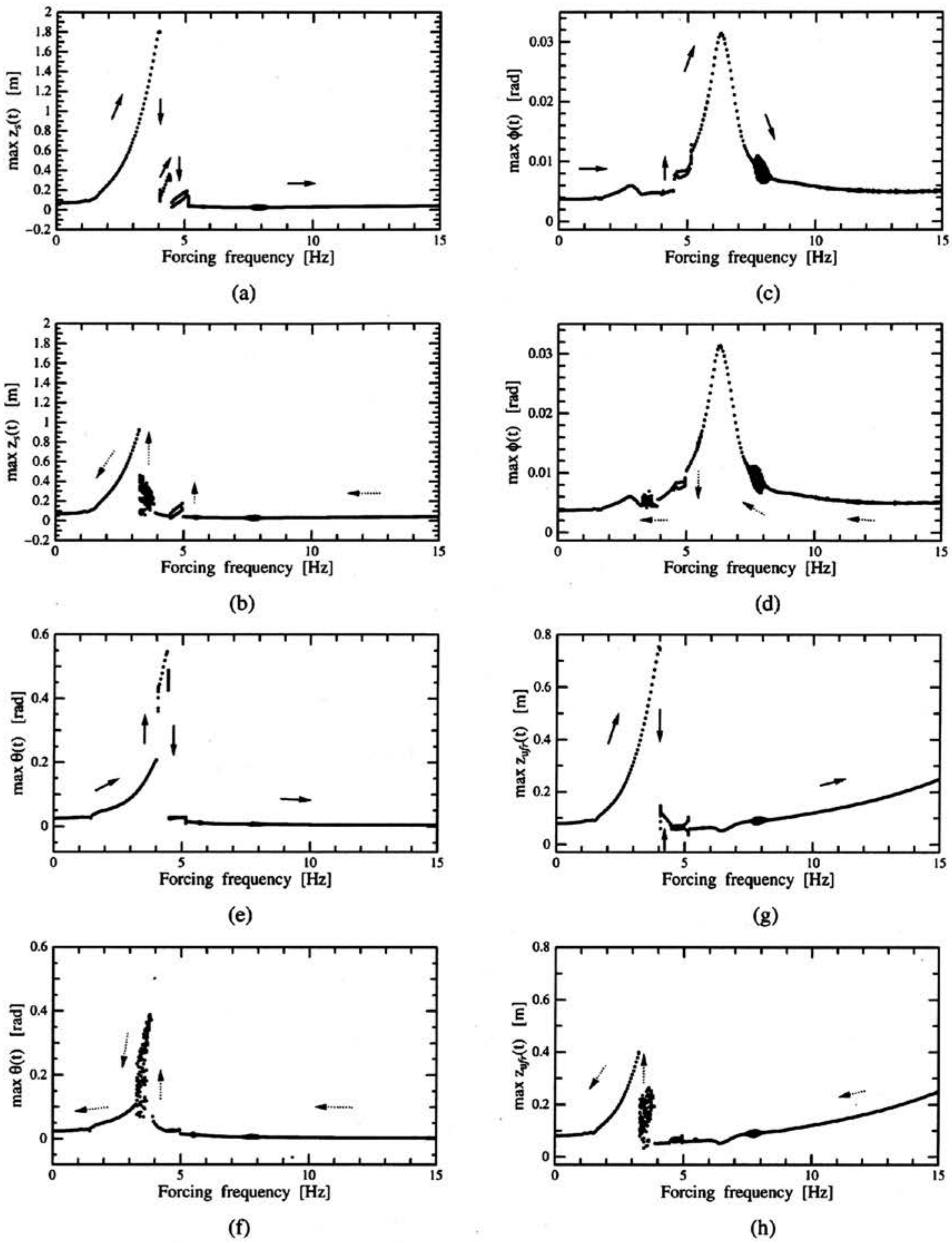

Fig. 2 Frequency-response diagrams when the forcing frequency f is slowly increased and decreased ($A = 0.08$ m, $\beta = 9°$, $\alpha = 58°$, $0 < f \leq 15$ Hz): (a),(b) $\max|z_s(t)|$; (c),(d) $\max|\phi(t)|$; (e),(f) $\max|\theta(t)|$; (g), (h) $\max|z_{uf\ell}(t)|$.

frequency is increasing, two jumps at $f = 4.00$ Hz, $f = 4.45$ Hz can be observed. With the increase of the frequency the oscillation changes into beats between $f = 7.55$ Hz and $f = 8.20$ Hz. As shown in Fig. 2(b), there are upward jumps at $f = 5.00$ Hz and $f = 3.30$ Hz as the forcing frequency decreases. The beats begin at $f = 8.00$ Hz and end at $f = 7.35$ Hz. An unstable region which does not exist as f is increasing appears in the forcing frequency $3.30 \leq f \leq 3.85$ Hz.

Since the chaotic motion can not only appear as forcing frequency is within or near the unstable regions with beats, but also as the frequency is near one where the jump phenomenon is observed, the heave motion of the unsprung mass may become chaotic as $3.30 \leq f \leq 3.85$, $7.55 \leq f \leq 8.20$ and around $f = 4.00$ Hz or $f = 4.45$ Hz for some initial conditions. This result can also be obtained by observing the other frequency response diagrams in Fig. 2.

To confirm the existence of chaotic response, the Poincaré maps as $f = 3.4$ Hz is given in Fig. 3 which show the strange attractors and indicate the motion is chaotic. The Fig. 3 shows that the motion of the system in different coordinate can

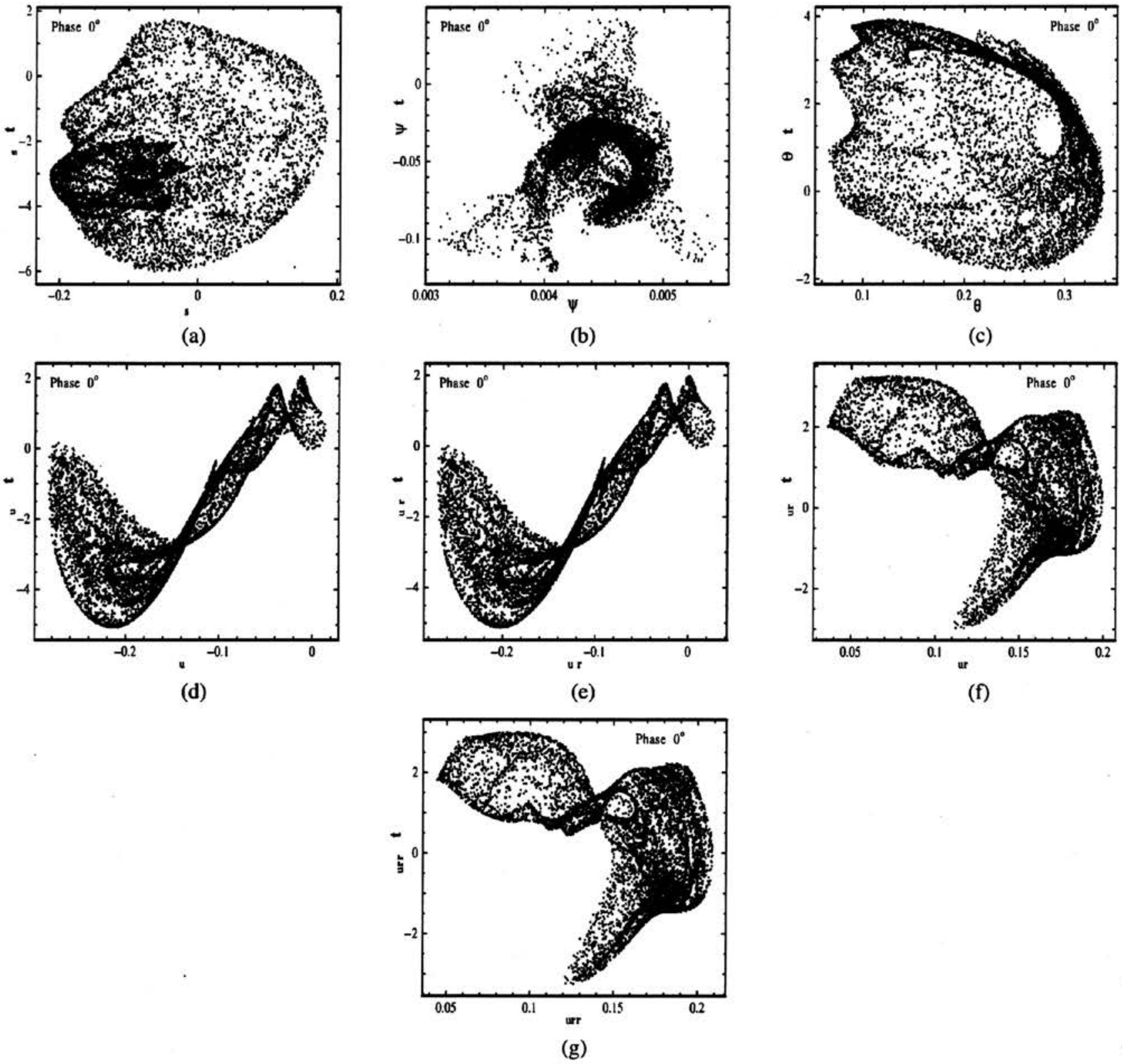

Fig. 3 Poincaré maps of chaotic motion of the system ($A = 0.08$ m, $f = 3.4$ Hz, $\beta = 9°$, $\alpha = 58°$).

become chaotic simultaneously even some motion is small, see Fig. 3(b).

Damping plays an important role in dynamic behavior of a nonlinear system since it can change the response of the system dramatically. To investigate the effect of damping to chaotic response, the factor of enlargement D_N is defined and taken as the bifurcation parameter. As D_N is changed, ever damping coefficient is multiplied by D_N. Therefore the damping coefficients of the vehicle model are enlarged or reduced by D_N times.

One of the bifurcation diagrams of the system is shown in Fig. 4. They were obtained by plotting the Poincaré points of the response against D_N. It is found that the responses of the system are chaotic as $0.5 \leq D_N \leq 1.6$, which means that the chaotic response exists even the damping coefficients are reduced to 50% or enlarged to 160%.

IV. Conclusions

The dynamic responses of a full ground vehicle model which is subjected to sinusoid disturbance with large amplitude are investigated through numerical simulation. The main conclusions are as follows.

- The chaotic responses exists in the system and the forcing frequencies for inducing chaos are in the unstable regions of the frequency response diagram.
- Generally, it is considered that the change of system parameters is an easy way of eliminating chaos. However, for the studied system, the dynamics are not sensitive to variation of damping coefficients if these coefficients are changed simultaneously. This result can be an good example to show the complexity of the nonlinear system.
- To avoid the chaotic response in dynamic design of a system, the simplest way is to change the system parameters. Thus the sensitivity of the system's parameters to chaos needs to be discussed and this is left for the further research.

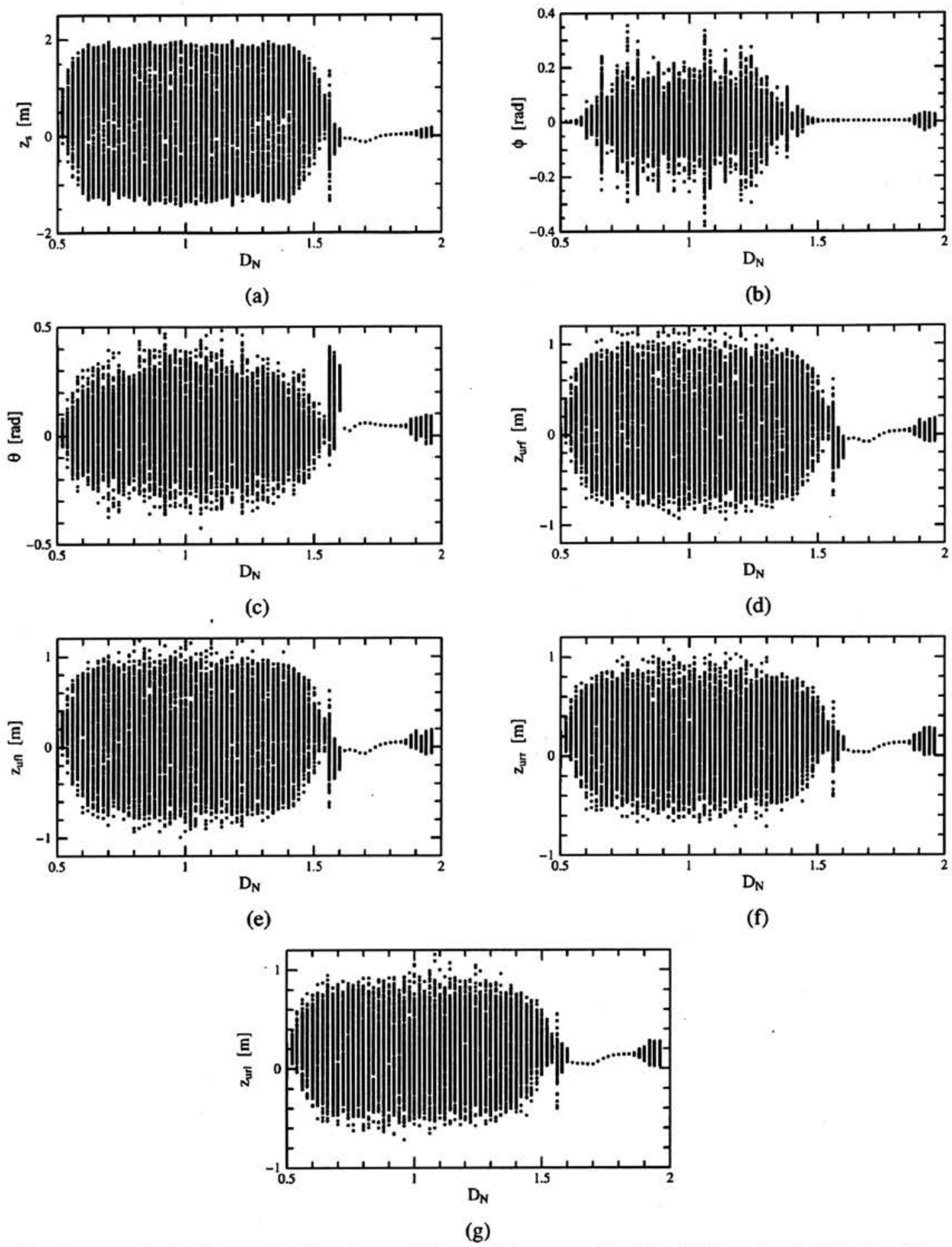

Fig. 4 Bifurcation diagrams obtained by varying damping coefficients of the system D_N ($A = 0.08$ m, $f = 3.4$ Hz, $\beta = 9^\circ$), $\alpha = 58^\circ$: (a) $z_s(t)$; (b) $\phi(t)$; (c) $\theta(t)$; (d) $z_{uf\ell}(t)$; (e) $z_{ufr}(t)$; (f) $z_{ur\ell}(t)$, and (g) $z_{urr}(t)$.

REFERENCES

[1] A. Moran and M. Nagai, Optimal Active Control of Nonlinear Vehicle Suspension Using Neural Networks, *JSME Int. J.*, Series C, Vol. 37 (1994), pp. 707–718.

[2] L. Půst, O. Szöllös, The forced chaotic and irregular oscillations of the nonlinear two degrees of freedom (2dof) system. *Int. J. of Bifurcation and Chaos* Vol. 9 (1999), 479–491.

[3] Q. Zhu and M. Ishitobi, Chaotic Behavior of a Nonlinear Vehicle Model: A Numerical Investigation, Recent Research Developments in Sound and Vibration, Transworld Research Network, S. G. Pandalai (Managing editor), pp. 363–372, 2002.

[4] Q. Zhu and M. Ishitobi, The Chaotic Vibration of a Nonlinear Full-Vehicle Model, *Int J. of Solids and Structures*, Vol. 43 (2006), pp. 747-759.

[5] F.C. Moon, Chaotic and Factal Dynamics: An Introduction for Applied Scientists and Engineers, 1st ed. John Willey & Sons Ltd., New York, 1992.

小山工業高等専門学校　機械工学科
E-mail : zhu@oyama-ct.ac.jp

(Received Sept,30,2009)